

Numeric simulation of the solidification of the pure iron varying the solidification process parameters

A.C. Mossi¹ and M.M. Pariona²

¹Profesor del Departamento de Matemática e Estadística y del Postgrado de Ingeniería e Ciencia de Materiales. ²Aluno de Iniciação Científica, Universidad Estadual de Ponta Grossa, Universidad Estadual de Ponta Grossa, Campus Uvaranas, Bloco CIPP, Laboratório Limac, CEP 84030-900, Uvaranas, Ponta Grossa - PR, Brasil. Fone (042) 220-3056.
E-mail: mmpariona@uepg.br

Abstract

In the study reported in this work, two-dimensional numerical simulations were made of pure iron solidification in industrial Al 50/60 AFS greensand and mullite molds, using the finite element technique and the ANSYS software program. For this purpose, the thermophysical properties of iron were considered temperature-dependent, while for sand and mullite these properties were considered constant, and the convection phenomenon was also considered on the external surface of the mold. In order to study the influences of the parameters in the solidification process, such as, sand and mullite mold types, preheating temperature of the mold (ambient and heated), superheating temperature of the liquid metal and loss of heat on the mold by convection, the optimization through the factorial design was accomplished. Metallurgical characteristics, such as the attack zone in the feed head and hot top, were not taken into account in this study, since they are irrelevant to the behavior of metal to mold heat transfer. Owing to the temperature-dependent thermo-physical properties of iron, this type of problem is of nonlinear characteristic. The results of the heat transfer are shown throughout the 2D system, as thermal flow, thermal gradient, the cooling curves at various points of the solidified specimen were determined, as well as the analysis of the factorial design of the result and heating or/and cooling in the molds were also accomplished. Through the analysis of the factorial design result of the parameters it was found which mold type influences negatively the result and the interaction of the metal temperature with the convection phenomenon contributed significantly to the result. The cooling curves characterize the grain size and mechanical properties of metal; hence, owing to the smaller grain size of metal cast in mullite molds, this type of mold grants better mechanical properties to the cast part.

Key words: Numerical simulation, finite elements, solidification of iron, sand and mullite molds.

Simulación numérica de la solidificación del hierro puro variando los parámetros del proceso de solidificación

Resumen

En este trabajo se realizó la simulación numérica en dos dimensiones de la solidificación del hierro en moldes de arena sintética al verde industrial, Al 50/60 y mulita por medio de la técnica de elementos finitos con el programa ANSYS. Las propiedades termofísicas del hierro fueron consideradas dependientes de la temperatura, mientras que estas propiedades para la arena y la mulita se consideraron constantes; adicionalmente, se tomó en cuenta el fenómeno de convección en la superficie externa del molde. Se estu-

dió el efecto de los siguientes parámetros en el proceso de solidificación: tipo de arena y mulita, temperatura de precalentamiento del molde (ambiente y calentado), temperaturas de supercalentamiento del metal líquido y la pérdida de calor por convección en el molde. La optimización de estos parámetros se realizó por el método de diseño factorial. Las características metalúrgicas del cabezal de alimentación y del tope caliente no se consideraron en este estudio, ya que son irrelevantes en el comportamiento de la transferencia de calor entre el metal y el molde. Debido a que las propiedades termofísicas del hierro dependen con la temperatura, este es un tipo de problema de característica no lineal. Los resultados de la transferencia de calor se presentan en un sistema de dos dimensiones para el flujo térmico, el gradiente térmico, las curvas de enfriamiento en varios puntos de la pieza solidificada y las curvas de calentamiento y/o enfriamiento en los moldes; así como también, el análisis de los resultados por el método de planeamiento factorial fueron realizados, pues, mediante esta análisis fue encontrado que el tipo de molde influencia negativamente en el resultado, por otro lado, la interacción de la temperatura del metal con el fenómeno de convección contribuyó significativamente en el resultado.

Palabras clave: Simulación numérica, elementos finitos, solidificación del hierro, moldes de arena y mulita.

Introduction

The technological difficulties involved in casting processes vary considerably according to the melting temperature characteristics of the metal, which in turn are related to the physicochemical properties and structures of metals and alloys. These difficulties also involve a series of properties, which include differences in chemical activities between the elements that constitute the alloy, solubility of the gases, method of solidification among the chemical elements, type of molding, and coefficients of solidification shrinkage [1, 2]. On the other hand, the cooling process is influenced by the flow of molten metal, the mold filling and properties of the metal, all these factors can produce variations in the geometrical dimensions, the shape of the surface finishing and the quality of the cast part [3].

The present study investigated the solidification of pure iron in industrial greensand molds, AI 50/60 AFS, and mullite molds (the latter material is frequently used in the Shaw process). The thermo-physical properties were considered as a function of the temperature, i.e., thermal conductivity and enthalpy. The properties of the sand and mullite were considered constant because these temperature-dependent properties were not found in literature. The presence of the convection phenomenon on the external surface of the mold was also taken into account. In order to study with more details the influences of the parameters in the solidification process, such as, sand and mullite mold types,

preheating temperature of the mold (ambient and heated), superheating temperature of liquid metal and heat loss on the mold for convection, a factorial design of these parameters to optimize the process was accomplished. This type of problem has a nonlinear characteristic and was solved by means of the finite element method and, to render the solution feasible, the convergence was controlled.

The purpose of this work was to make a comparative study of the different types of molds, varying those parameters. As a result, heat transfer was observed in the cast metal, at the interface and in the mold, as well as cooling curves at different points in the cast metal, beyond that, heating and cooling curves at different points in the mold. Thus, the microstructural quality and mechanical properties of the cast part depend not only on the casting technique employed, but also on the characteristics and properties of the molding process and cast metal used.

Numerical Simulation

Solidification is accompanied by the release/absorption of latent heat at the solid-liquid and solid-solid interfaces. Consequently, solidification process involves phase changes, in this case, the enthalpy method is the more appropriated modeling to describe this process, because in this method the latent heat is inserted in enthalpy, which represents the phase transformation. Then, the differential equation of thermal flow for the transient nonlinear state that de-

scribes this phenomenon was presented as proceeds [4-6]:

$$K \left(\frac{\partial^2 T}{\partial x^2} + \frac{\partial^2 T}{\partial y^2} + \frac{\partial^2 T}{\partial z^2} \right) = \frac{dh}{dt}, \tag{1}$$

where the enthalpy, $h = \int \rho c dT$ subject to the convective boundary condition:

$$q = K \frac{\partial T}{\partial x} \Big|_{x=0} = K \frac{\partial T}{\partial y} \Big|_{y=0} = K \frac{\partial T}{\partial z} \Big|_{x=0} = h_f (T - T_{\text{ambiente}}). \tag{2}$$

where q is the heat, K is the thermal conductivity, c is the specific heat, and ρ is the density of the material. These properties may be temperature-dependent, in which case equation (1) is transformed into a nonlinear transient equation. h_f is the coefficient of convective heat transfer on the mold's external surface, T is the temperature, and T_B is the temperature of the environment.

Through equations (1) and (2) one can determine the distribution of temperature or transfer of heat during the process of solidification in the casting of pure iron in sand or mullite molds. In this case, the solution of those equations were considered in 2-D.

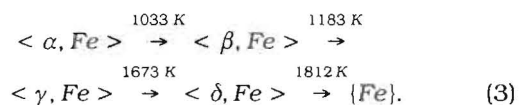
Methodology of the Numerical Simulation

The finite element method studied by several authors [6-10]. Software programs were used to simulate the solidification of pure iron in

greensand and mullite molds, with the aid of a Pentium III 1GHz microcomputer. The following procedures were adopted for the simulations:

- a. The geometric project for sand or mullite mold is illustrated in Figure 1 (a), which represents the symmetry in three-dimensions, showing the entry of the cast metal in the upper part of the figure. The simulation did not consider the positioning of the feed head, hot top and conventional book mold model normally used. The symmetry was used in order to reduce the number of grid points, i.e., to facilitate the computation of the system of nonlinear equations and avoid overloading the computer's capacity. However, in this work the solution of Equations (1) and (2) was made for half symmetry in 2-D, which is illustrated in Figure 1 (b).
- b. A selection of the types of materials was made then, in this case, pure iron and sand or mullite.

The phase transformation in pure iron may be represented as follows [11],



The properties, such as, specific heat (C_p) and latent heat (ΔH) are shown for pure iron in function of the temperature (T). They are shown as follow [11]:

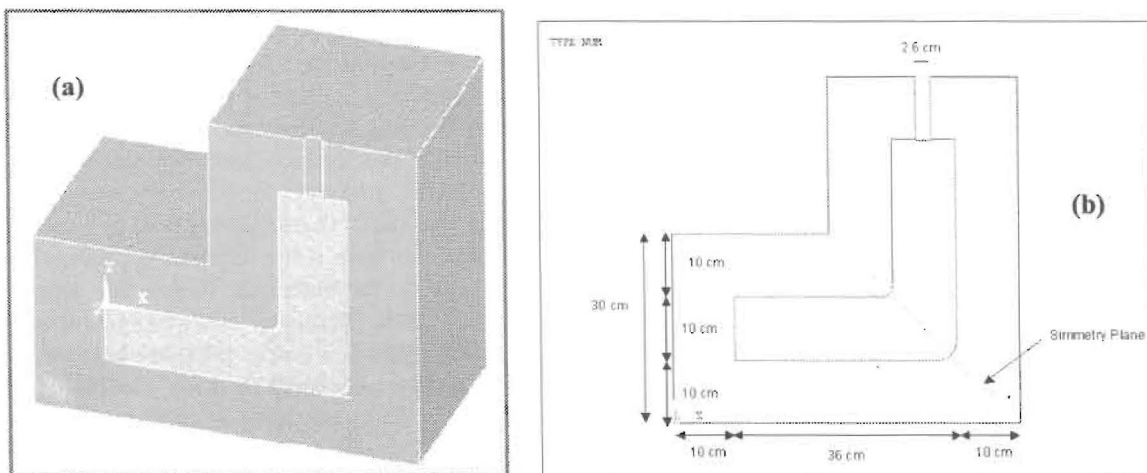


Figure 1. Symmetry of the cast part and mold in 3-D and 2-D.

$$\begin{aligned}
 C_{P, \langle \alpha\text{-Fe} \rangle} &= 17,49 + 24,77 \times 10^{-3} T \text{ J/K.mol}, \\
 C_{P, \langle \beta\text{-Fe} \rangle} &= 37,66 \text{ J/K.mol}, \\
 C_{P, \langle \gamma\text{-Fe} \rangle} &= 7,70 + 19,50 \times 10^{-3} T \text{ J/K.mol}, \\
 C_{P, \langle \delta\text{-Fe} \rangle} &= 43,93 \text{ J/K.mol}, \\
 C_{P, \{\text{Fe}\}} &= 41,84 \text{ J/K.mol}, \langle \alpha\text{-Fe} \rangle \rightarrow \langle \beta\text{-Fe} \rangle; \\
 \Delta H_{1033}^{\circ} &= 2761,4 \text{ J/mol}, \langle \beta\text{-Fe} \rangle \rightarrow \langle \gamma\text{-Fe} \rangle; \\
 \Delta H_{1183}^{\circ} &= 690,4 \text{ J/mol}, \langle \gamma\text{-Fe} \rangle \rightarrow \langle \delta\text{-Fe} \rangle; \\
 \Delta H_{1673}^{\circ} &= 690,4 \text{ J/mol and } \langle \delta\text{-Fe} \rangle \rightarrow \{\text{Fe}\}; \\
 \Delta H_{1812}^{\circ} &= 15,355 \text{ J/mol.} \quad [4]
 \end{aligned}$$

Density of pure iron = 7870 Kg/m³,
atomic weight = 0.056 Kg/mol.

Through these data, the enthalpy was calculated for pure iron, as shown in Table 1. Also in this table the properties of sand and mullite are shown. Thermal conductivity for pure iron was approximate, according to the data of AISI-SAE 1008 steel [12, 13].

- c. For process optimization, the factorial design of the parameters was accomplished, just as they are shown in Table 2 [2].
- d. The initial and boundary conditions were then applied to the symmetry of the parts according with Table 2. The boundary condition was the convection phenomenon generated by the natural aerated environment. This phenomenon was applied to the outside walls of the sand or mullite mold. This phenomenon is represented by Equation (2) and the coefficient of convective heat transfer, as shown in Table 2. The effects of the application of refractory paint and of the gassing process were not taken into consideration either.

The final step consists in solving the problem of heat transfer of the mold - cast metal system, using Equations (1) and controlled by the convergence condition. The result of the heat transfer is shown in 2-D, as well as the heat flux, the thermal gradient, the cooling curves in different points in the cast metal, and the heating and cooling curves in different points in the mold.

Results and Discussion

The numerical simulation of solidification using the ANSYS 9 software program [11] was performed for a pure iron corner piece in an industrial greensand mold, AI 50/60, dry, and in a mullite mold as illustrated in Figure 1. The results were showed after 1.5 hours of solidification, for which the increment of each substep of time was 5 seconds.

The work of numerical simulation was accomplished according with Table 2, for each line of it the simulation was accomplished. In Figure 2 the results of heat transfer are shown for lines 2 and 10. These results are more relevant for these lines, because the solidification temperatures that correspond to these lines are the smallest for sand and mullite respectively. In Figure 2 the distributions of the temperatures can be observed in the whole system in both molds, as well as in the cast metal (where the numbers inside the graphs represent temperatures in degrees K), after 1.5 hour of solidification. The results showed a difference for temperature distribution in both systems. Comparing graphs (a) and (b), the sand mold presented a range of temperature variation between 391 and 1198 K and the mullite mold presented a range of 626 and 751 K, consequently, in the sand mold there was a larger range of temperature variation, the justification is that the mullite presents high thermal conductivity and density in relation to the mold of sand (to see Table 2), this resulted couldn't be compared with the literature, because it was not found. Observing the cast metal, shown in graphs (c) and (d) in more detail, in it is also noticeable that a larger range of temperature variation happened inside the sand mold. That is because the physical properties of the molds are different in thermal conductivity and density, especially the thermal conductivity, which influences the most the solidification process. It is also noticeable that the maximum points (MX) of temperature for both cast metals are located in points a little displaced from one another, and that the minimum points (MN) are located in different positions, although these points should be located in the same position as in graph (c). This point (MN) in graph (d) suffered a displacement; this could be due to some type of minimum numeric mistake, as it can be observed in the

Table 1
Properties of pure iron, sand and mullite [12-16]

Temperature (K)	Enthalpy (MJ/m ³)	Temperature (K)	Thermal conductivity W/(m.K)
298	0	273	59.5
373	200.75	373	57.8
473	498.87	473	53.2
573	831.83	746	49.4
673	1199.61	673	45.6
773	1602.22	773	41.0
873	2039.65	873	36.8
973	2511.91	973	33.1
1033	3200.23	1073	28.1
1073	3412.0	1273	27.6
1183	4120.86	1473	29.7
1273	4453.89		
1373	4849.96		
1473	5273.45		
1573	5724.36		
1673	6299.75		
1812	9317.24		
1812	9676.0		

Density (kg/m ³)	7880
Melt temperature	1812 K

Properties of the industrial sand, Al 50/60 AFS	
Specific heat	1172.3 J/(Kg.K)
Thermal conductivity	0.52 W/(m.K)
Density	1494.71 kg/m ³

Properties of mullite	
Specific heat	1172.3 J/(kg.K)
Thermal conductivity	5.86 W/(m.K)
Density	3100 kg/m ³

graphs, this mistake can be due to the time substep size and to the abrupt variations of the properties of the molds, maybe in this case, the time substep size can be more appropriate if smaller than 5 seconds, however, the time of processing has been long.

In Figure 3, the result of the thermal flow is presented for both systems, in magnitude, shown in graphs (a) and (b), as well as in vectorial form, in graphs (c) and (d). Through these graphs it can be observed that a larger thermal flow happened in the sand mold than in the mullite mold. In both

Table 2
Factorial design of the solidification process parameters

	1° Mold Sand (-) Mullite (+)	2° Mold temp. 298 K (-) 423 K (+)	3° Metal temp. 1823 K (-) 1912 K (+)	4° Convection phen. (h_p) 5 (W/m ² K) (-) 25 (W/m ² K) (+)	Temperature after 1.5 h of solidification
1	-	-	-	-	1284.76
tbl2	-	-	-	+	1186.04
3	-	-	+	-	1330.68
4	-	-	+	+	1230.48
5	-	+	-	-	1338.37
6	-	+	-	+	1225.19
7	-	+	+	-	1405.6
8	-	+	+	+	1282.23
9	+	-	-	-	907.57
10	+	-	-	+	743.36
11	+	-	+	-	936.90
12	+	-	+	+	767.84
13	+	+	-	-	984.42
14	+	+	-	+	807.55
15	+	+	+	-	1004.41
16	+	+	+	+	829.32

systems it is noticeable that the maximum point (MX) of thermal flow is located at the same point, however, the minimum (MN) of the thermal flow is a little dislocated. In this figure it can be observed that the largest magnitude of the thermal flow corresponds to the minimum point (MN) of the temperature distribution (Figure 2), because at this point the solidification begins. Besides, in graphs (c) and (d) of Figure 3, the vectors indicate the largest variation of thermal flow; this could be due to a lesser thickness of the mold influenced by the convection phenomenon.

In addition, the thermal gradients were determined for both systems. The result is presented in Figure 4, in magnitude and in vectorial form. As it can be seen in the graph, the thermal gradient is larger in the sand mold than in the mullite mold, that is, due to that, the conductivity of the sand is much smaller in relation to the mullite mold. Also, the maximum and minimum

thermal gradients are located exactly at the same points that the thermal flow happened. In this case, it is noticeable in graphs (c) and (d), that the direction of the thermal gradient is contrary to the thermal flow. The direction of the thermal gradient corresponds to the direction of the solidification, from the cold zone to the hot zone.

According to Table 2, the most representative result for the solidification time of 1.5 h was that corresponding to lines 2 and 7 for the sand mold, line 2 corresponding to the smallest solidification temperature (118.4 K), in this case, the mold temperature was that of the environment, the liquid metal was considered without superheating and it was considered high loss of heat on the mold by convection (25 W/(m²·K), and line 7 corresponds to the largest solidification temperature (1405.6 K), in this case, the temperature of the mold was preheated (423 K), liquid metal was superheated (80 K).

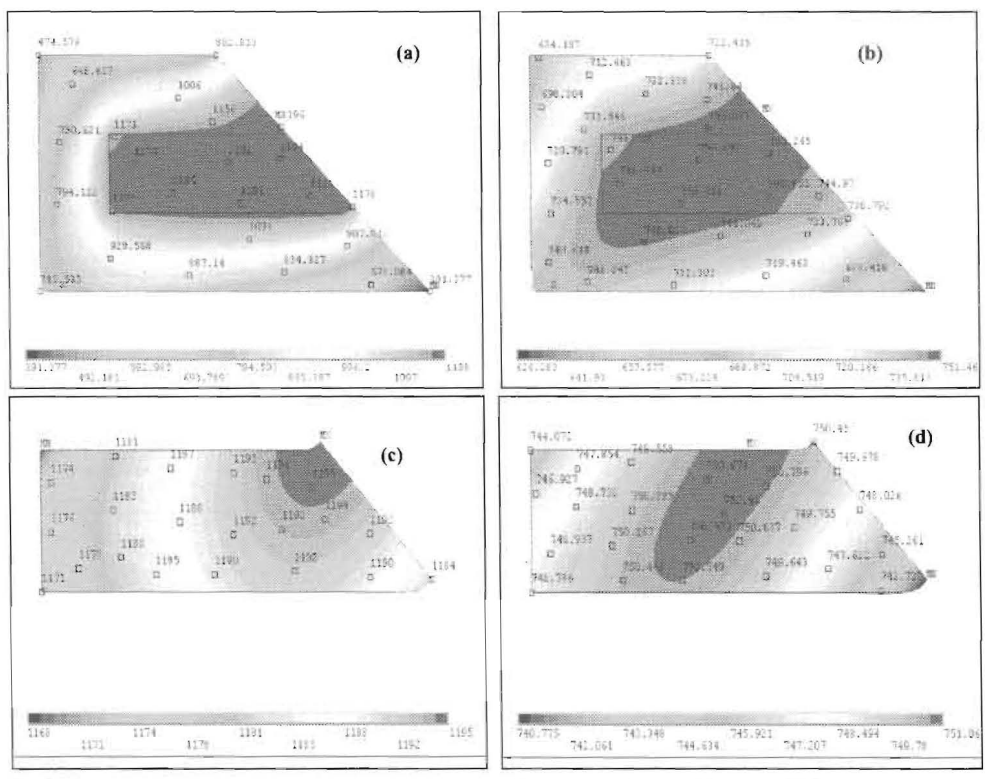


Figure 2 Temperature distribution in (a) sand mold system, (b) mullite mold system, (c) cast metal in a sand mold and (d) cast metal in a mullite mold.

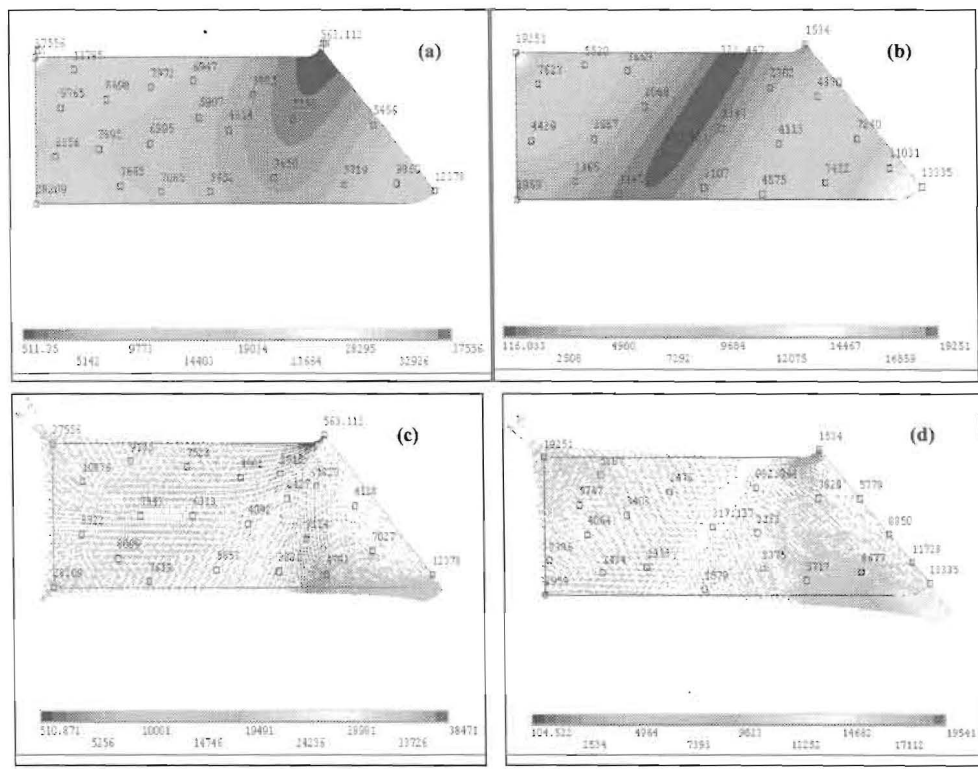


Figure 3. Heat flux in magnitude and in vectorial form, as in cast metal in a sand and a mullite molds.

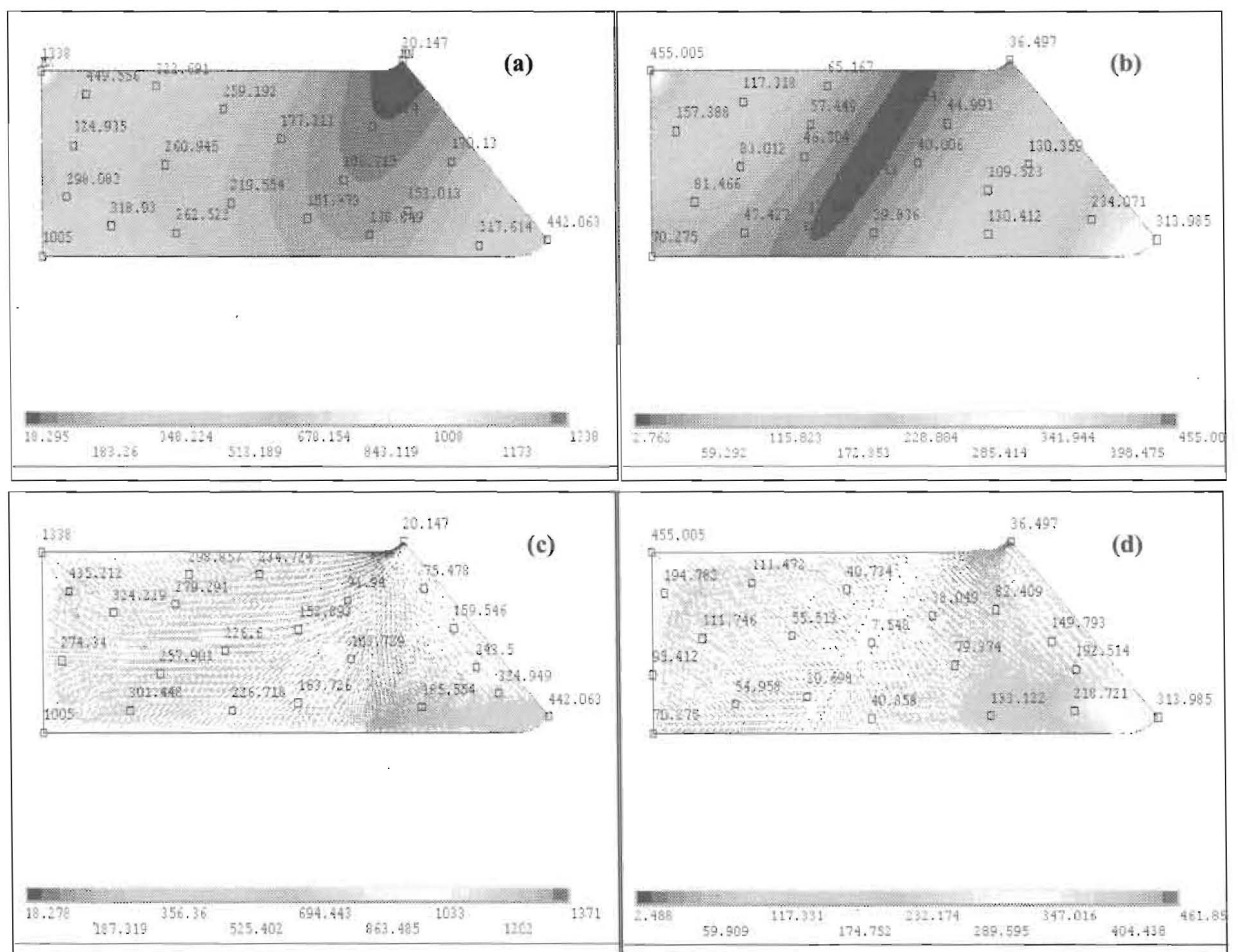


Figure 4. Thermal gradient in magnitude and in vectorial form, as in cast metal in a sand and a mullite molds.

Lines 10 and 15 were relevant for the mullite mold, line 10 corresponding to the smallest solidification temperature (743.36 K), where, it was established without preheating the mold, it was also established without superheating the liquid metal; a strong loss of heat on the mold by convection ($25 \text{ W}/(\text{m}^2 \cdot \text{K})$) has happened, and line 15 corresponds to the largest solidification temperature (1004.41 K), because the preheating temperature of the mold was (423 K), high superheating temperature of the liquid metal (80 K) was fixed and loss of heat in the mold by convection ($5 \text{ W}/(\text{m}^2 \cdot \text{K})$) was established. According to the result, a larger cooling in the mullite mold than in the sand mold was observed, because the physical properties of the materials are different, especially the thermal conductivity of the mullite influences. Obviously, for the conditions without

preheating the mold and without superheating the liquid metal and for a strong loss of heat in the mold due to the convection phenomenon, consequently these conditions generated slower solidification temperatures as much in the sand mold as in the mullite mold (lines 2 and 10).

Inside the cast metal some points were numbered, these points are shown in Figure 5. At these points the cooling curves were determined, that is shown in Figure 6. The data of the last column of Table 2 present the solidification temperature after 1.5 h of solidification. Observing in more detail Figure 6, in the sand mold the phase change of Fe- δ to Fe- γ happened, around the temperature of 1673 K, but, the other phase changes didn't happen. In the mullite mold, the phase change was not very well defined, that is, it de-

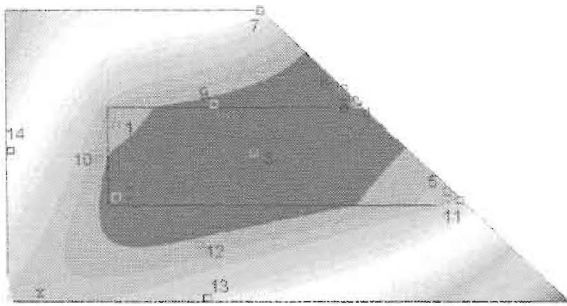


Figure 5. Reference points as much for the sand as for mullite systems.

depends on the situation of the design and properties of this material. For instance, for line 10, the phase change of Fe- β to Fe- α happened around 1060 K, at the other points the phase transformation happened at the temperature of 947 K, for

this temperature does not correspond to the transformation given by equation (3), this temperature could correspond to supercooling phenomenon. For line 15, phase transformation exists at some points, for instance, of Fe- γ to Fe- β for the temperature of 1158 K and in the other points happened the transformation of Fe- β to Fe- α in 1033 K. On the other hand, the phase transformation for high temperatures did not happen. The result of phase change of iron during the cooling in different molds was not possible of to corroborate with the literature, for this study type was not found in the literature, because even this research type is relatively new.

In this work, the solidification process in the cast metal and the processes of heating and cooling in the molds were also studied. For this purpose, Figure 5 was considered, for both sys-

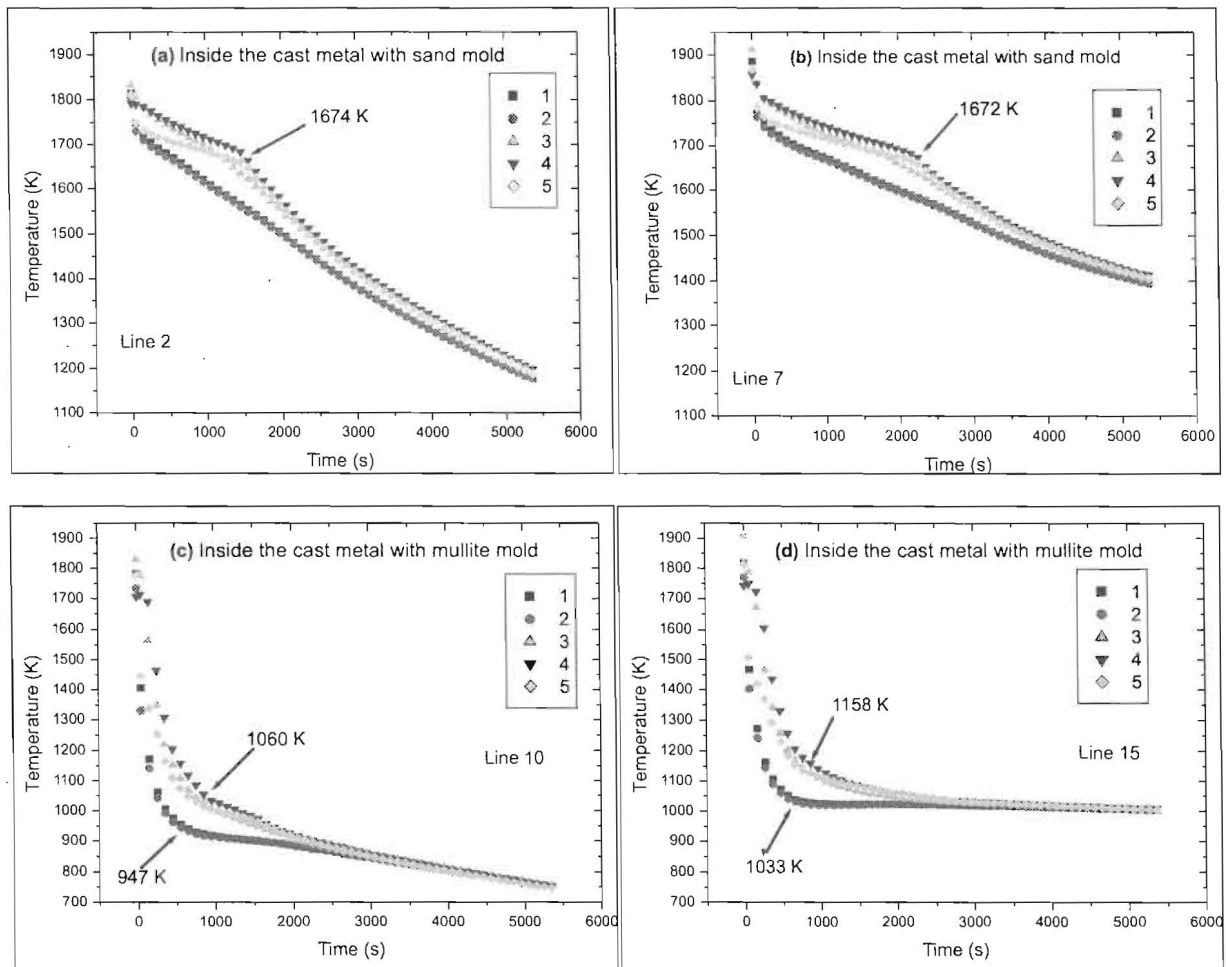


Figure 6. Cooling curves of cast metal in sand and in mullite molds.

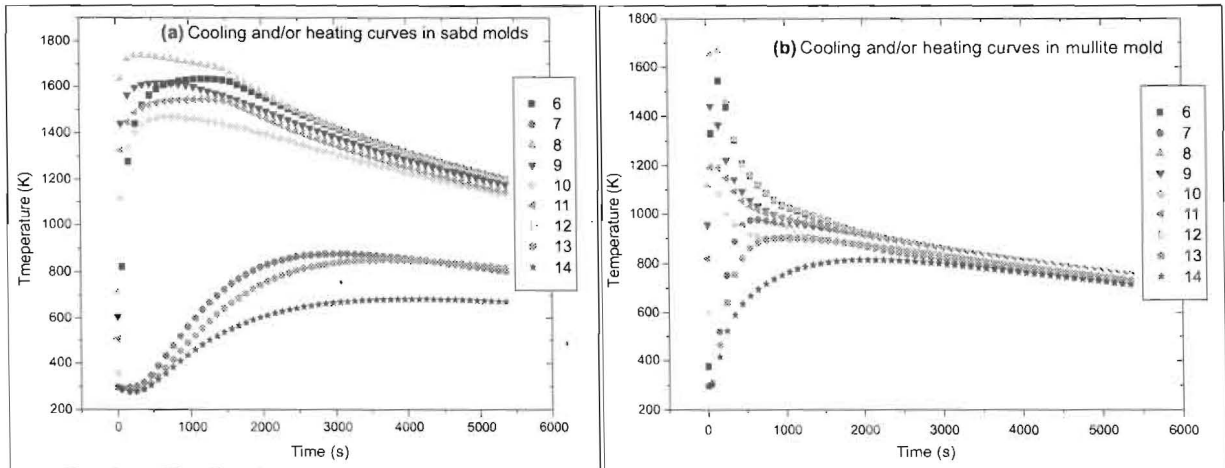


Figure 7. Cooling and/or heating curves in sand and in mullite molds.

tems the same points were selected inside the cast metal (1, 2, 3, 4 and 5), in order to study the solidification process, and the points inside the mold (6, 7, 8, 9, 10, 11, 12, 13 and 14), in order to study the heating and/or cooling process. Inside the cast metal that corresponds to the sand mold, the cooling curves for the solidification process were show in Figure 7. The phase changes were observed at the points where the cooling is slower. When the cooling is fast, it is not possible to observe the curvatures of phase change. Possibly, the phase transformation is controlled by the diffusion phenomenon, when the cooling velocity is slow, the curvature of phase change can be observed.

The heating and cooling curves are presented in the curves (a) of Figure 7 for the sand mold, where the points 6, 8, 9, 10 and 11 present the heating and cooling behavior, because, these points are near the cast metal. However, at points 7, 12, 13, and 14 only the heating behavior comes, because these points are moved away of the cast metal. In Figure 7(b) the heating and cooling curves are presented in the mullite mold, at points 6, 8, 9, 10 and 11 the abrupt heating is presented, and the cooling presents an accentuated fall, compared with the sand mold. On the other hand, in the points 7, 12, 13 and 14 only the cooling curves are presented, because they are moved away from the cast metal. It is observed in both systems; all the cooling curves tend to converge, being this convergence faster for the mullite mold.

Finally the analysis of the factorial design result of the parameters was accomplished considering that this involves the solidification process (last column of Table 2), being this result correspondent to the smallest temperature after 1.5 h of solidification. This analysis is presented in Figure 8. Observing this figure, the moved away points of the straight line are the ones that have larger influences in the result, for instance, point 1 (mold type) influences negatively in this result, because, especially the sand mold was observed, which presented a larger temperature after of 1.5 h of solidification. Another important point was 34, it means the interaction of the metal temperature with the convection phenomenon, this interaction contributed significantly to the result.

Conclusions

This study is a comparative work of the numeric simulation, by the finite element method, of the process of solidification of pure iron in sand and in mullite molds, during 1.5 h of solidification. Results in 2D were obtained, such as heat transfer, thermal flow, thermal gradient, cooling curves during the solidification process, factorial design of the result and heating or/and cooling in the molds during the solidification process. The result was completely different in both systems. This can be due to the fact that these molds have different physical properties. Therefore, cooling

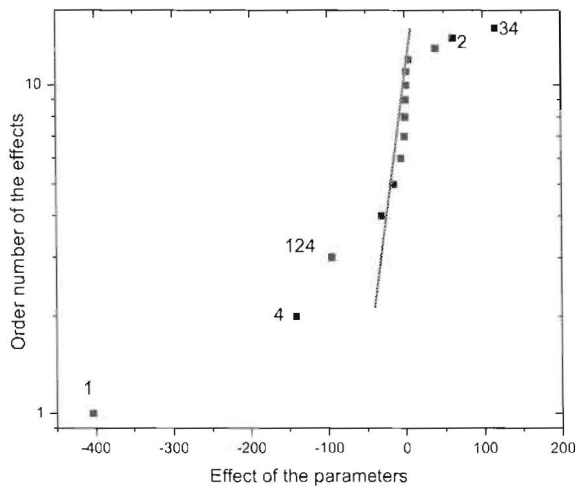


Figure 8. Result of the factorial design of the solidification process parameters.

in the sand system was slower than in the mullite system. This fact caused a larger thermal flow and thermal gradient in the sand system than in the mullite system. These phenomena happened especially in the cold zone of the cast metal, where the solidification begins. It was also observed that, in the convergence process, the mullite system needed a larger iteration number, probably because it reached lower temperatures than the sand system, during the same time of solidification. In the cooling curves, at several points the sand system presented phase changes, however, this did not happen in the mullite system. This phenomenon can be explained by the fact that in the sand system the cooling is slower than in the mullite system, possibly in the sand system the diffusion phenomenon prevails. Through the analysis of the factorial design result of the parameters it was found which mold type influences negatively in the result and the interaction of the metal temperature with the convection phenomenon contributed significantly to the result. The cooling curves characterize the grain size and mechanical properties of metal; hence, owing to the smaller grain size of metal cast in mullite molds, this type of mold grants better mechanical properties to the cast part. The cooling and/or heating in the molds was also studied, and in the mullite mold the heating and cooling are abrupt, but all the curves in both systems tend to converge.

References

1. Guo Z., Saunders N., G.N., Miodownik A.P. and . Schillé J.-Ph "Modelling of materials properties and behaviour critical to casting simulation", *Materials Science and Engineering A* 413-414 (2005) 465-469.
2. Pariona M.M., Bolfarini C., dos Santos R.J. and Kiminami C.S.: "Application of Mathematical Simulation and Factorial Design Method to the Optimization the Atomization Stage in the Forming of a Cu-6% Zn Alloy", *Journal of Materials Processing Technology*, v.102, n.1, (2000) 221-229.
3. Ivaldo L., Ferreira A., Spinelli J.E., Pires J.C. and Garcia A. "The effect of melt temperature profile on the transient metal/mold heat transfer coefficient during solidification", *Materials Science and Engineering A* 408 (2005) 317-325.
4. Liu B.C., Kang J.W. and Xiong S.M.: "A study on the Numerical Simulation of Thermal Stress During the Solidification of Shaped Casting", v.2, (2001) 57-164.
5. Katarov I.H.: "Finite Element Modeling of the Porosity Formation in Casting", *International Journal of heat and Mass Transfer*, v.46, (2003) 1545-1552.
6. Su X.: "Computer Aided Optimization of an Investment bi-metal Casting Process", Ph.D. Thesis, University of Cincinnati, Department of Mechanical, Industrial and Nuclear Engineering, 2001.
7. ASM Handbook, "Casting" v.15, The materials Information Society, 1996.
8. Ansys, "Heat Transfer 9 Training-Manual", Ansys, Inc., Canonsburg, PA, 2004.
9. Grozdanic V.: "Numerical simulation of the solidification of a steel rail-wheel casting and the optimum dimension of the riser", *Materiali in tehnologije*, v. 36, (2002) 39-41.
10. Santos, C.A., Fortaleza E.L., Ferreira C.R.L., Spim J.A. and Garcia A. "A solidification heat transfer model and a neural network based algorithm applied to the continuous casting of steel billets and blooms", *Modelling Simul. Mater. Sci. Eng.* 13 (2005) 1071-1087.

11. Handbook Ansys 9.0, Ansys, Inc., Canonsburg, PA, 2004.
12. Upadhyaya G.S. and Dube R.K.: "Problems in Metallurgical Thermodynamics and Kinetics", Pergamon Press, Oxford, 1977.
13. Metal Handbook, ninth ed., v.1, "Properties and Selection: Iron and Steel", American Society for Metals, Ohio, 1978.
14. Kingery W. D.; Bowen R. K. and Uhlmann H. K.: "Introduction to Ceramics", 2nd ed., John Wiley, New York, 1976.
15. Hertzberg R.W.: "Deformation and Fracture Mechanics of Engineering Materials", John Wiley & Sons, New York, 1996.
16. Ozisik M.N.: "Heat Transfer a Basic Approach", McGraw-Hill, New York, 1985.

Recibido el 08 de Marzo de 2005

En forma revisada el 11 de Septiembre de 2006